

University of Nebraska - Lincoln

DigitalCommons@University of Nebraska - Lincoln

Biological Systems Engineering: Papers and Publications

Biological Systems Engineering

2020

Glucocorticoid Priming of Nonviral Gene Delivery to hMSCs Increases Transfection by Reducing Induced Stresses

Andrew Hamann

Tyler Kozisek

Kelly Broad

Angela K. Pannier

Follow this and additional works at: <https://digitalcommons.unl.edu/biosysengfacpub>



Part of the [Bioresource and Agricultural Engineering Commons](#), [Environmental Engineering Commons](#), and the [Other Civil and Environmental Engineering Commons](#)

This Article is brought to you for free and open access by the Biological Systems Engineering at DigitalCommons@University of Nebraska - Lincoln. It has been accepted for inclusion in Biological Systems Engineering: Papers and Publications by an authorized administrator of DigitalCommons@University of Nebraska - Lincoln.

Glucocorticoid Priming of Nonviral Gene Delivery to hMSCs Increases Transfection by Reducing Induced Stresses

Andrew Hamann,¹ Tyler Kozisek,¹ Kelly Broad,¹ and Angela K. Pannier¹

¹Department of Biological Systems Engineering, University of Nebraska-Lincoln, Lincoln, NE 68583-0726, USA

Human mesenchymal stem cells (hMSCs) are under study for cell and gene therapeutics because of their immunomodulatory and regenerative properties. Safe and efficient gene delivery could increase hMSC clinical potential by enabling expression of transgenes for control over factor production, behavior, and differentiation. Viral delivery is efficient but suffers from safety issues, while nonviral methods are safe but highly inefficient, especially in hMSCs. We previously demonstrated that priming cells with glucocorticoids (Gcs) before delivery of DNA complexes significantly increases hMSC transfection, which correlates with a rescue of transfection-induced metabolic and protein synthesis decline, and apoptosis. In this work, we show that transgene expression enhancement is mediated by transcriptional activation of endogenous hMSC genes by the cytosolic glucocorticoid receptor (cGR) and that transfection enhancement can be potentiated with a GR transcription-activation synergist. We demonstrate that the Gc-activated cGR modulates endogenous hMSC gene expression to ameliorate transfection-induced endoplasmic reticulum (ER) and oxidative stresses, apoptosis, and inflammatory responses to prevent hMSC metabolic and protein synthesis decline, resulting in enhanced transgene expression after nonviral gene delivery to hMSCs. These results provide insights important for rational design of more efficient nonviral gene delivery and priming techniques that could be utilized for clinical hMSC applications.

INTRODUCTION

Because of their roles in wound healing,¹ trophic tissue support,^{2,3} and immunomodulation,⁴ along with their differentiation ability⁵ and immune-privileged status,^{6,7} human mesenchymal stem cells (hMSCs) are under study for cell and gene therapeutics,⁸ as well as tissue engineering and regenerative medicine.⁹ In addition to their natural healing and regenerative potentials, safe and efficient gene delivery to hMSCs could further endow these cells with beneficial properties for cell therapies.¹⁰ For example, hMSCs can be engineered to express pro-survival genes,^{11,12} adhesion ligands targeting specific cell-membrane receptors,^{13–15} lineage-specific genes for directed differentiation,^{16,17} or genes that encode for the production and secretion of growth factors,^{18,19} cytokines,^{20,21} and microRNA (miRNA)

in exosomes.^{22,23} Thus, researchers are investigating methods to efficiently transfer genes to hMSCs.

Viral delivery is efficient but suffers from safety issues related to immunogenicity and insertional mutagenesis,^{24,25} as well as small transgene capacity and difficult design and scale-up.²⁶ Nonviral methods typically deliver plasmid DNA (pDNA) with lipid or polymer transfection reagents that condense DNA to nanosized complexes that are capable of crossing cell membranes and facilitating *in vitro* transfection.²⁷ Nonviral methods overcome many of the shortcomings of viral delivery but suffer from low efficiency, especially in hMSCs. For example, optimized transfection of hMSCs with the commercially available Lipofectamine (LF) 2000 results in only 10%–30% of cells being successfully transfected,^{28–31} and the ubiquitously used 25-kDa branched polyethylenimine (PEI) is only able to achieve about 20% transfection.^{31–33} In addition, both lipid- and polymer-based transfections are associated with significant toxicity in hMSCs,^{34,35} limiting both transgene expression levels and downstream therapeutic efficacy. Therefore, more efficient and less toxic nonviral gene delivery methods to hMSCs are needed to advance their therapeutic potential.

Previously, to both improve and better understand the biology of nonviral gene delivery, our work has focused on pharmacologically “priming” cells for increased transgene expression³⁶ by modulating relevant molecular pathways that are important to the biological processes involved in gene delivery.^{37,38} Specifically, we demonstrated in hMSCs transfected with pDNA lipoplexes, that the glucocorticoid (Gc) dexamethasone (DEX) increases transgenic luciferase activity about 10-fold, increases transgenic enhanced green fluorescent protein (EGFP) mean fluorescence intensity of EGFP-positive (EGFP+) cells about 2-fold, increases transfection efficiency about 3-fold (i.e., percentage of EGFP+ transfected cells), and increases the duration of transgene expression, all relative to unprimed transfected hMSCs.³⁹

Received 11 February 2020; accepted 17 July 2020;
<https://doi.org/10.1016/j.omtm.2020.07.014>.

Correspondence: Angela K. Pannier, Department of Biological Systems Engineering, University of Nebraska-Lincoln, 231 L.W. Chase Hall, Lincoln, NE 68583-0726, USA.

E-mail: apannier2@unl.edu



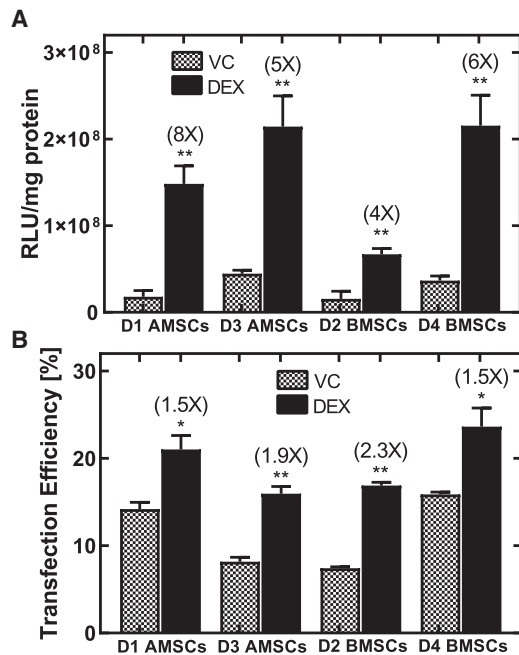


Figure 1. Priming hMSCs with the Gc Drug DEX Significantly Enhances Nonviral Gene Delivery

(A and B) 150 nM DEX treatment 25 min prior to transfection with lipid reagent, Lipofectamine (LF) 3000, complexed with pDNA encoding a fusion protein of luciferase and enhanced green fluorescent protein (EGFP), increased (A) transgenic luciferase expression from 4- to 8-fold as measured in relative light units normalized per milligram of cellular protein (RLU/mg protein) and (B) increased transfection efficiency (i.e., the proportion of hMSCs expressing EGFP) by about 2-fold as quantified by fluorescent microscopy, all relative to vehicle control (VC) treatment, in D1 AMSCs, D3 AMSCs, D2 BMSCs, and D4 BMSCs. Data are plotted as mean \pm SEM ($n = 3$). Asterisks denote significance to VC conditions: * $p \leq 0.05$; ** $p \leq 0.01$. Fold change increase over VC conditions.

It was also shown that binding of the glucocorticoid receptor (GR) was required for the Gc-mediated enhancement and that DEX ameliorated the decrease in metabolic activity induced by transfection of hMSCs.³⁹ Recently, we also demonstrated that enhanced transfection by Gc priming, in both bone-marrow-derived hMSCs (BMSCs) and adipose-derived hMSCs (AMSCs) derived from multiple donors, is not the result of increased cellular or nuclear pDNA internalization, or of messenger RNA (mRNA) transcription, but that Gc rescues hMSCs from transfection-induced apoptosis and protein synthesis decline.⁴⁰ In this work, we further investigate the potential mechanisms by which Gc priming enhances hMSC transfection by exploring how DEX and other specific GR modulators affect transgene expression as well as endogenous pathways related to GR action and nonviral gene delivery.

RESULTS

Gc Priming Enhances Nonviral Gene Delivery to hMSCs

First, to again demonstrate that Gc priming can enhance nonviral gene delivery to hMSCs, BMSCs and AMSCs derived from multiple human donors (denoted as donor number or, hereinafter,

D[number]) (Table S1) were “primed” for transfection by treatment with 150 nM DEX or ethanol vehicle control (VC) 25 min prior to delivery of LF 3000 complexed with pEGFP-Luc plasmid expressing a fusion protein of EGFP and luciferase. DNA lipoplexes had an average diameter of $1,016 \pm 76$ nm and an average zeta potential of 15.4 ± 0.5 mV. Treating hMSCs with DEX increased transgenic luciferase expression from 4- to 8-fold over VCs, depending on donor and tissue source, measured in luminescence relative light units (RLUs) normalized to total protein (RLUs per milligram of protein), and DEX increases were statistically significant in all four donors, relative to VCs ($p \leq 0.01$) (Figure 1A). Treatment with DEX also increased transfection efficiency (i.e., the proportion of hMSCs expressing EGFP) from 1.5- to 2.3-fold over VCs, and DEX increases were statistically significant in all four donors, relative to VCs ($p \leq 0.05$) (Figure 1B). We next aimed to explore the molecular mechanisms by which Gc priming enhances hMSC transfection. Since the GR can exist within either the membrane or the cytoplasm, we first investigated which GR type mediates transfection priming in hMSCs.

Gc Transfection Enhancement Is Mediated by Binding of Cytosolic GR

Our lab has demonstrated that Gc priming of hMSC transfection enhancement is mediated by binding of Gc to the GR, as treatment with the GR antagonist RU486 prevented transfection enhancement by DEX.³⁹ In order to determine whether the membrane-bound GR (mGR) or cytosolic (cGR) is involved in the enhancement of transfection by Gc treatment, hMSCs were either treated with membrane-impermeable bovine serum albumin (BSA)-conjugated cortisol (BSA-Cort; Cort covalently linked to BSA at a density of about 30 Cort molecules per BSA molecule) or with cell-permeable unconjugated (free) BSA and cortisol (Cort) as a control. BSA-Cort can bind mGR but cannot cross cell membranes to bind cGR,⁴¹ whereas free Cort can bind mGR and cross cell membranes to bind cGR. When hMSCs were primed with 0.5 μ M or 1 μ M BSA-Cort 25 min prior to transfection with pEGFP-Luc complexed with LF reagents, luciferase transgene expression was not significantly enhanced over VCs, while 0.5 μ M or 1 μ M free unconjugated Cort with BSA was able to significantly enhance transgene expression between 3- and 14-fold over VCs in D1, D2, and D3 BMSCs, as well as D1 AMSCs ($p \leq 0.05$) (Figure 2). Failure of BSA-Cort to increase transgene expression over VCs suggests that the cGR, a transcription factor that activates and represses endogenous gene expression, must be bound for Gc to enhance transfection in hMSCs and that mGR, which exerts its effects via non-genomic signaling pathways,⁴¹ is not involved in pathways that increase hMSC transfection. We next aimed to explore by what mechanisms the cGR enhances hMSC transfection.

Gc Transfection Enhancement Is Mediated by GR Gene Transcription Activation

Since cGR activated by Gc is known to exert its effects by both activation and repression of specific gene transcription, we primed hMSCs with varying concentrations of either DEX or compound A (CpdA), a “dissociated Gc” that induces the GR to repress but not

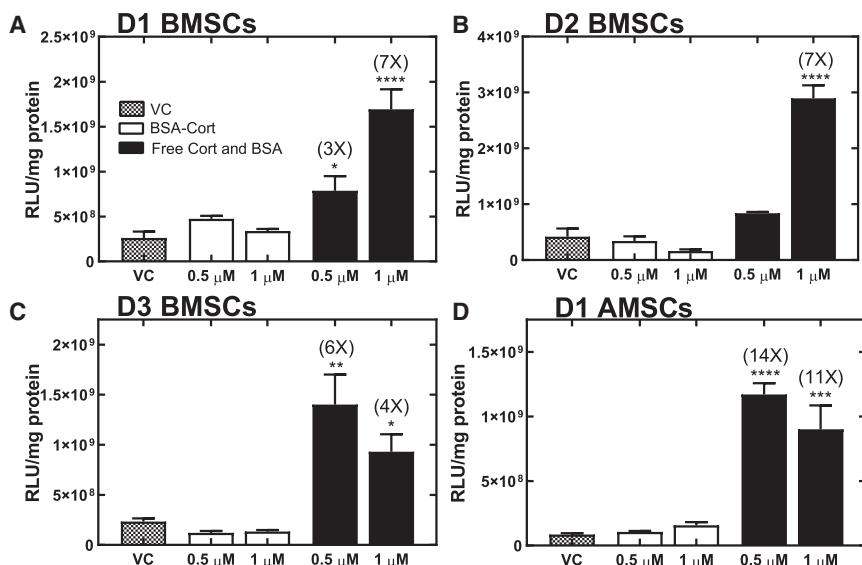


Figure 2. Cell-Impermeable Glucocorticoid Does Not Enhance hMSC Transfection

Cell-permeable free cortisol (Cort), capable of binding cytosolic glucocorticoid receptor (cGR), delivered with bovine serum albumin (BSA) significantly increases transgenic luciferase expression in transfected hMSCs over the VC, but membrane-impermeable BSA-Cort conjugate, only capable of binding membranous (mGR), does not increase luciferase expression. hMSCs were primed with compounds 25 min prior to transfection with lipid-pDNA complexes and lysed for analysis after 48 h. (A–D) Free Cort treatment resulted in 3- to 14-fold increases in transgene expression, normalized to total cellular protein, over VC in (A) D1 BMSCs, (B) D2 BMSCs, (C) D3 BMSCs, and (D) D1 AMSCs. Data are plotted as mean \pm SEM ($n = 3$) of luciferase luminescence relative light units per milligram of total protein (RLU/mg protein). Asterisks denote significance to VC conditions: * $p \leq 0.05$; ** $p \leq 0.01$; *** $p \leq 0.001$; **** $p \leq 0.0001$. Fold change increase over VC conditions.

activate gene transcription.⁴² When hMSCs were treated 25 min prior to transfection, DEX (10 nM to 1 μ M) significantly increased transgenic luciferase expression over VCs ($p \leq 0.01$), while CpdA (10 nM to 10 μ M) did not increase luciferase expression over VCs, in transfected D2 BMSCs, D3 BMSCs, D1 AMSCs, and D2 AMSCs (Figure 3). Failure of CpdA to increase hMSC transgene expression suggests that Gc priming enhances nonviral gene delivery as a result of GR activation, but not repression, of the transcription of specific endogenous hMSC genes. We next hypothesized that, if activation of endogenous genes by cGR mediates hMSC transfection enhancement, a known synergist of GR transcriptional activation may be able to further increase transgene expression over Gc priming alone.

Gc Transfection Enhancement Can Be Potentiated by Inhibiting GR Nuclear Exit

Since the aforementioned studies suggest that Gc enhances nonviral gene delivery through activation of endogenous gene transcription by cGR, we hypothesized that this enhancement could be increased further with nuclear exportin 1 (XPO1) inhibitor KPT-330 (KPT), a drug that has been shown to synergistically increase GR nuclear residence and transcriptional activation.⁴³ Priming hMSCs with 150 nM DEX and KPT (100 nM to 1 μ M) 25 min prior to transfection significantly increased transgenic luciferase expression from 2- to 4-fold over priming with DEX alone ($p \leq 0.05$) in D1 BMSCs, D2 BMSCs, D3 BMSCs, D1 AMSCs, and D2 AMSCs (Figures 4 and S1). In addition, priming with 1 μ M KPT alone did not significantly increase transgene expression over no-priming controls ($p > 0.05$) in D1 AMSCs, D4 AMSCs, D1 BMSCs, and D4 BMSCs (Figure S1). After demonstrating that hMSC transfection enhancement by Gc priming is mediated by the activation of endogenous genes by GR and further enhanced by a known synergist of GR transcriptional activation, we next aimed to investigate what GR-modulated pathways may influence hMSC transfection.

Gc Ameliorates hMSC Oxidative Stress Induced by Transfection

Since it is known that transfection can induce cell stresses, our previous work showed that Gc ameliorates hMSC apoptosis induced by transfection,⁴⁰ and our results in the previous sections implicate GR transcriptional activation as a potential mechanism of Gc transfection priming, we next measured the effect of transfection and Gc priming on hMSC oxidative stress by fluorescently staining cellular reactive oxygen species (ROS) 48 h after transfection. Transfection of hMSCs when primed with only VC significantly increased the proportion of cells positively stained for ROS 4- to 5-fold over that of untransfected hMSCs, ($p \leq 0.0001$), whereas priming with 150 nM DEX 25 min prior to transfection significantly decreased the proportion of cells positively stained for ROS to about half that of VCs ($p \leq 0.001$) in D4 BMSCs, D1 AMSCs, D2 AMSCs, and D3 AMSCs (Figure 5). Given that Gc priming ameliorated hMSC oxidative stress induced by transfection, we next studied specific endogenous genes that GR activation of transcription may modulate to improve hMSC health and enhance their transfection.

Transfection and Gc Modulates Expression of Endogenous Genes Related to ER Stress, Apoptosis, Oxidative Stress, and Inflammation in hMSCs

To further elucidate mechanisms of transfection and Gc priming in hMSCs, we investigated the expression of specific endogenous genes related to transfection and GR action. Specifically, we quantified mRNA expression of genes related to endoplasmic reticulum (ER) stress, apoptosis, oxidative stress, and inflammation by qRT-PCR, 24 h after transfection, when transgene production and toxicity become evident in hMSCs. Transfection of hMSCs when only primed with VC upregulated the ER stress-induced and apoptosis mediator, CCAAT-enhancer-binding protein homologous protein (CHOP), from 2- to 4-fold relative to untransfected cells, and this increase was statistically significant in D1 AMSCs

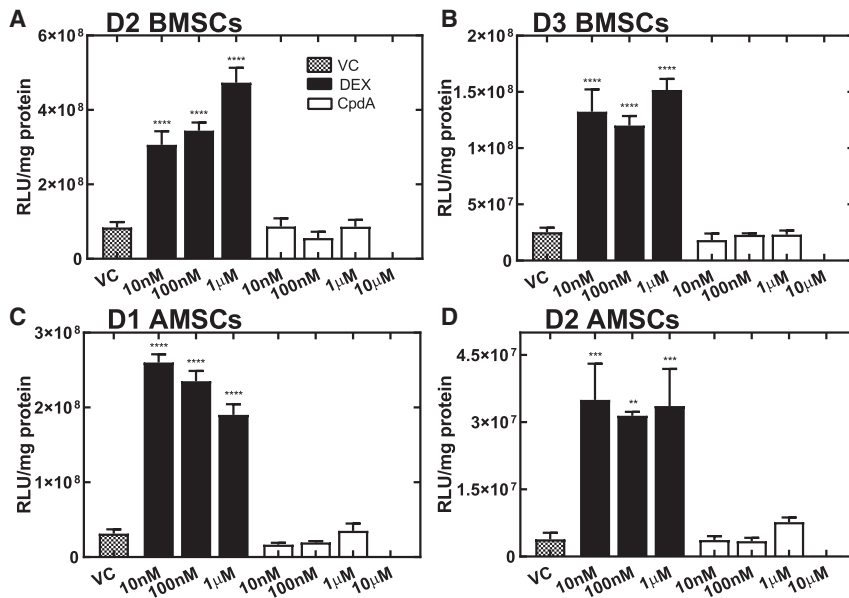


Figure 3. hMSC Transfection Is Not Enhanced by Glucocorticoid without Transcription-Activation Properties

DEX, which induces GR to both induce and repress endogenous gene transcription, significantly increases transgenic luciferase expression in transfected hMSCs over the VC, but CpdA, which only induces GR to repress endogenous gene transcription, does not increase luciferase expression over VC. hMSCs were primed with compounds 25 min prior to transfection with LF 3000 pDNA complexes and lysed for analysis after 48 h. (A–D) D1 BMSCs (A); D3 BMSCs (B); D1 AMSCs (C); and D2 AMSCs (D). Data are plotted as mean \pm SEM ($n = 3$) of luciferase luminescence relative light units per milligram of total protein (RLU/mg protein). Asterisks denote significance to VC conditions: ** $p \leq 0.01$; *** $p \leq 0.001$; **** $p \leq 0.0001$. Fold change increase over VC conditions.

($p \leq 0.05$) and D2 AMSCs ($p \leq 0.0001$) (Figure 6A). However, transfected hMSCs primed with DEX had CHOP expression levels that were downregulated relative to VC, and this decrease was statistically significant in D1 AMSCs ($p \leq 0.05$) and D2 AMSCs ($p \leq 0.001$) (Figure 6A). Furthermore, expression of the antioxidant gene metallothionein was upregulated 2- to 5-fold by transfection (in the presence of VC) relative to untransfected hMSCs, and this increase was statistically significant in D2 BMSCs ($p \leq 0.001$) and D3 BMSCs ($p \leq 0.01$) (Figure 6B). Metallothionein expression was further upregulated by DEX priming relative to VC-primed hMSCs, and this increase was statistically significant in all donors ($p \leq 0.01$) (Figure 6B). Additionally, expression of the inflammatory cytokine interleukin-6 (IL-6), was significantly upregulated in all VC-primed transfected hMSCs from 10- to 40-fold relative to untransfected cells ($p \leq 0.05$) (Figure 6C). DEX priming downregulated IL-6 expression relative to VC-primed transfected cells, and this decrease was statistically significant in D2 BMSCs ($p \leq 0.0001$), D1 AMSCs ($p \leq 0.05$), and D2 AMSCs ($p \leq 0.05$) (Figure 6C). Finally, inflammatory enzyme cyclooxygenase-2 (COX2) expression was significantly upregulated in all transfected VC-primed hMSCs from 10- to 60-fold, relative to untransfected cells ($p \leq 0.05$) (Figure 6D). DEX priming downregulated COX2 expression relative to transfected VC primed hMSCs, and this decrease was statistically significant in D2 BMSCs ($p \leq 0.05$), D3 BMSCs ($p \leq 0.05$), and D1 AMSCs ($p \leq 0.05$) (Figure 6D). Taken together, the results of these endogenous gene expression studies suggest that hMSC transfection induces ER stress and apoptosis (CHOP), oxidative stress (metallothionein), and inflammatory (IL-6 and COX2) pathways, and the expression of these genes (and, thus, these processes) is reduced to levels closer to that of untransfected cells, through gene activation by GR after Gc priming, resulting in improved cell health and subsequent transgene expression.

DISCUSSION

This work explored the mechanisms by which Gc-bound GR enhances nonviral gene delivery to hMSCs. The Gc priming effect on hMSC transfection is robust and consistent, as evidenced by significant increases in total transgenic luciferase expression from both BMSCs and AMSCs derived from multiple human donors (Figure 1A), as well as significant increases in transfection efficiency (i.e., proportion of hMSCs expressing transgene) (Figure 1B). Gc enhancement of hMSC transfection reported in this work is consistent with our previous demonstration of about 10-fold increases in total luciferase expression^{39,40} and about 2-fold increases in transfection efficiency.³⁹

Most Gc effects are mediated by binding of GR, and we previously demonstrated that binding of GR is required to mediate Gc priming enhancement of hMSC transfection, as pre-treatment with the GR antagonist RU486 abrogated enhancement by DEX.³⁹ Since GR can exist either as a cytosolic inducible transcription factor (i.e., cGR) or as a membrane-bound receptor that exerts its effects via non-genomic signaling pathways (i.e., mGR),⁴¹ we investigated here which receptor was involved in hMSC transfection enhancement by priming with Gc that was either cell permeable or cell impermeable. Previous studies have successfully used BSA-conjugated Gc to discriminate between specific activities of cGR and mGR,^{41,44–46} and here cell-permeable free Cort significantly enhanced hMSC transgene expression, while cell-impermeable BSA-Cort conjugate did not (Figure 2), implicating cGR in the hMSC Gc transfection priming mechanism. Since Gc-bound cGR is transported to and translocated into nuclei, it has been suggested that Gc may enhance transfection by increasing nuclear pDNA accumulation,⁴⁷ but we previously demonstrated that DEX priming did not increase pDNA cellular or nuclear internalization or transgene transcription, in hMSCs,³⁸ leading us to next explore the effect of Gc priming on hMSC expression of endogenous genes related to transfection.

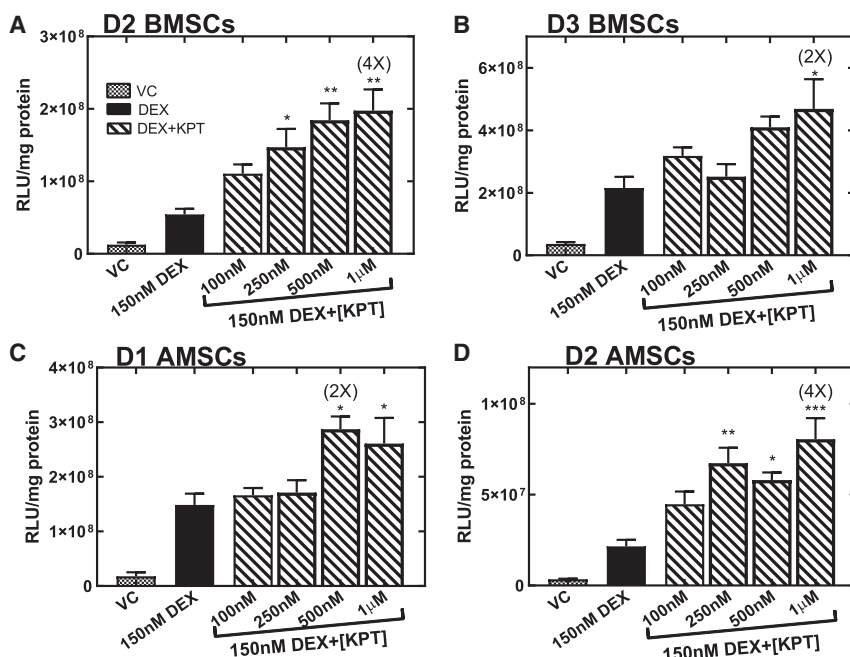


Figure 4. DEX Transfection Priming Is Potentiated by Compound that Inhibits GR Nuclear Export

(A–D) 150 nM DEX increases transgenic luciferase expression in transfected hMSCs over VC; and 150 nM DEX with varying doses of KPT-330 (KPT), a compound that inhibits nuclear export of the GR, significantly increases transgene expression from 2- to 4-fold over DEX alone in (A) D2 BMSCs, (B) D3 BMSCs, (C) D1 AMSCs, and (D) D2 AMSCs. hMSCs were primed with compounds 25 min prior to transfection with LF 3000 pDNA complexes and lysed for analysis after 48 h. Data are plotted as mean \pm SEM ($n = 3$) of luciferase luminescence relative light units per mg of total protein (RLU/mg protein). Asterisks denote significance to 150 nM DEX-alone conditions: * $p \leq 0.05$; ** $p \leq 0.01$; *** $p \leq 0.001$. Fold change increase over 150 nM DEX-alone conditions.

Since cGR exerts its effects through both repression and activation of endogenous gene transcription, we primed hMSCs with Cpda, a “dissociated” Gc that has been shown to repress the expression of inflammatory genes by causing GR to inhibit pro-inflammatory transcription factors similarly to DEX but that, in contrast with DEX, does not induce DNA binding and transcription from GR-targeted genes.^{42,48,49} Cpda’s inability to increase transfected hMSC transgene expression over VCs, as DEX priming does (Figure 3), suggests that DEX-bound GR enhances nonviral gene delivery through transcriptional activation, but not repression, of specific endogenous genes related to hMSC transfection. We further explored the ability of the GR to activate endogenous gene expression to prime hMSC transfection by treating with both DEX and KPT. KPT is an inhibitor of XPO1, which has been shown to increase GR nuclear residence and transcriptional activation.⁴³ Priming of KPT and DEX was able to further enhance hMSC transgene expression 2- to 4-fold over DEX alone (Figure 4), suggesting that a transfection strategy utilizing combinatorial priming could result in hMSC transgene expression sufficient for some clinical applications. KPT and DEX combinatorial priming enhanced transgene expression over DEX alone, presumably by increasing transcriptional activation of endogenous genes that modulate relevant hMSC transfection pathways, which we explored further in subsequent studies.

Since nonviral gene delivery has been shown to induce cellular stresses,^{37,50} and we have previously demonstrated that DEX priming of hMSCs prevents the transfection-induced decline of metabolism³⁹ and protein synthesis⁴⁰ and reduces transfection-induced apoptosis,⁴⁰ we investigated the effect of hMSC transfection and Gc priming on the production of ROSs, which are common mediators of cell stress and are produced by multiple cells when exposed to cationic

lipids^{51,52} and polymers⁵³ used for gene delivery. Transfection significantly increased ROSs in hMSCs over untransfected cells, and DEX priming of transfection significantly decreased ROSs relative to VC (Figure 5). Transfection-induced oxidative stress and apoptosis, as well as declining metabolism and protein synthesis in hMSCs, could be linked to ER stress,^{54,55} since ER stress can cause ROS generation and apoptosis and directly attenuates protein translation.⁵⁶ Given the relationship between gene delivery, Gc treatment, ER and oxidative stresses, apoptosis, and inflammation, we next quantified the expression of specific stress-associated genes in response to transfection and DEX priming in hMSCs.

Transfection strongly upregulated the ER stress-induced and apoptosis mediator CHOP gene⁵⁷ relative to untransfected hMSCs, while DEX priming with transfection significantly attenuated CHOP upregulation relative to transfection without DEX priming (Figure 6A). Transfection-induced ER stress likely causes the sharp decline in protein synthesis and increased apoptosis induced by transfection of hMSCs, which is attenuated by DEX priming in hMSCs.⁴⁰ Other studies have shown that hMSCs are vulnerable to ER stress-induced apoptosis after transplantation,^{58,59} and DEX has been shown to modulate ER stress responses in other cell types by promoting correct protein folding⁶⁰ and trafficking⁶¹ and by preventing apoptosis.⁶² Gc has also been shown to improve recombinant protein production in Chinese hamster ovary (CHO) cells by reducing protein aggregation through upregulation of genes that modulate oxidative conditions,⁶³ suggesting a connection between hMSC transfection, DEX priming, ER stress, apoptosis, and oxidative stress. DEX priming also strongly upregulated expression of the antioxidant protein metallothionein⁶⁴ (Figure 6B), which likely explains DEX priming’s ability to ameliorate hMSC oxidative stress that is induced by transfection. Finally, like oxidative stress, inflammatory responses are commonly linked to ER stress.^{65–68} In our gene expression studies, inflammatory cytokine IL-6 and enzyme COX2 were also strongly induced by transfection and downregulated by DEX priming (Figures 6C and 6D), which likely influenced the ability of hMSCs to recover

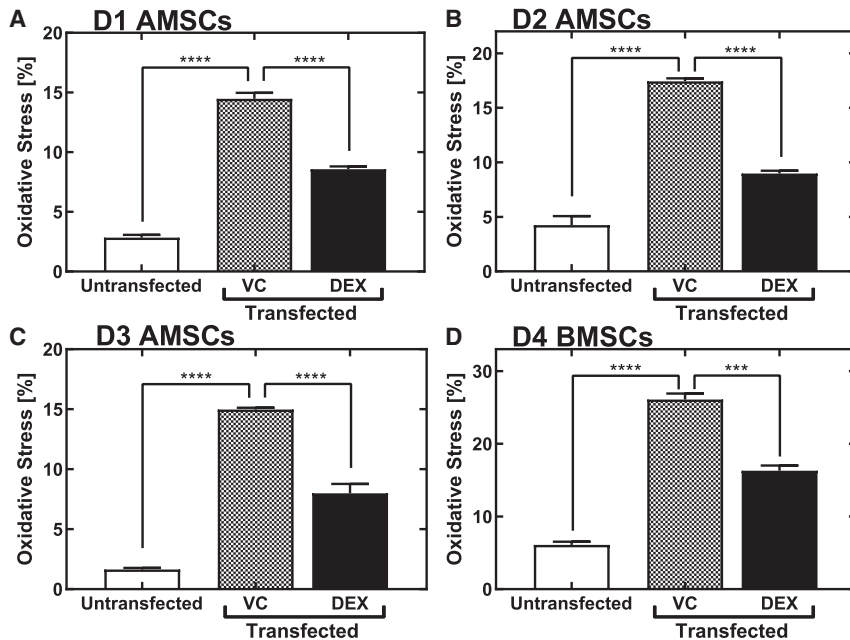


Figure 5. DEX Priming Decreases hMSC Oxidative Stress Induced by Transfection

(A–D) hMSCs were either untreated, transfected with 150 nM DEX priming, or transfected with VC priming. After 48 h, cellular reactive oxygen species (ROS) and nuclei were stained to calculate the fraction of hMSCs experiencing oxidative stress using fluorescent microscopy in (A) D1 AMSCs, (B) D2 AMSCs, (C) D3 AMSCs, and (D) D4 BMSCs. Data are plotted as mean \pm SEM ($n = 3$). Asterisks denote significance to designated conditions: *** $p \leq 0.001$; **** $p \leq 0.0001$.

from ER stress. Taken together, our gene expression studies suggest that transfection in hMSCs induces ER stress, which contributes to oxidative stress, apoptosis, attenuation of protein synthesis, and inflammatory response, all of which are attenuated by DEX priming to allow for increased transgenic protein production relative to unprimed transfected hMSCs.

In summary, this work reiterates that Gc priming of hMSC transfection significantly enhances transgene expression and suggests that enhancement is mediated by transcriptional activation of endogenous genes by cGR. In addition, we show that transfection enhancement can be further increased with the XPO1 inhibitor KPT, potentially by increasing cGR nuclear residence and transcriptional activity. Taken with our previous results,³⁸ this work demonstrates that transfection in hMSCs induces toxicity through ER and oxidative stresses, apoptosis, and inflammatory responses, which result in decreased cell metabolism and protein synthesis. Gc priming reduces these transfection-induced stresses to prevent the decline of hMSC metabolism and protein synthesis, resulting in increased transgene expression. Future work should focus on new priming strategies that address the effects of transfection-induced ER and oxidative stresses, apoptosis, and inflammatory responses toward developing safe and efficient gene delivery protocols for clinical hMSC applications.

MATERIALS AND METHODS

Cell Culture

BMSCs were purchased at passage 2 from Lonza (Walkersville, MD, USA) or acquired at passage 1 from the Texas A&M Institute for Regenerative Medicine Health Science Center College of Medicine (Bryan, TX, USA). All BMSCs were positive for CD29, CD44, CD105, and CD166 cell-surface markers and negative for CD14, CD34, and CD45. AMSCs were purchased at passage 1 from Lonza

and were positive for CD13, CD29, CD44, CD73, CD90, CD105, and CD166 and negative for CD14, CD31, and CD45 cell-surface markers. All human cells were acquired with informed consent using established ethical methods approved by the appropriate authorities. All experiments and methods were performed in accordance with relevant guidelines and regulations. All experimental protocols were approved

by the University of Nebraska-Lincoln Institutional Biosafety Committee. See Table S1 for BMSC and AMSC donor information. All cells were expanded and cultured in Minimum Essential Medium Alpha (MEM α ; GIBCO, Grand Island, NY, USA) supplemented with 10% heat-inactivated fetal bovine serum (FBS; GIBCO), 6 mM L-glutamine (GIBCO), and 1% penicillin-streptomycin (Pen-Strep; 10,000 U/mL; GIBCO) and incubated at 37°C with 5% CO₂. At 80% confluence, cell media were removed, and cells were washed with 1 \times phosphate buffered saline (PBS) and dissociated with 0.25% trypsin-ethylenediaminetetraacetic acid (EDTA; GIBCO); then, an equal volume of growth medium was added, and cells were pelleted to remove trypsin-EDTA, resuspended, and counted with trypan blue staining and a hemocytometer before diluting in growth medium (for transfection studies, as described next) or medium with 5% dimethyl sulfoxide (DMSO) to 6 \times 10⁴ cells per milliliter for freezing in 1-mL aliquots stored in liquid nitrogen.

For transfection experiments, after dissociation and counting as described earlier, hMSCs were seeded into 48- or 96-well plates (Corning Life Sciences, Corning, NY, USA) at passages 3 through 6, at 6,000 cells per square centimeter, allowed to adhere for 48 h until about 80% confluence, and then transfected as described later.

Priming Reagents

DEX and Cort were purchased from Sigma-Aldrich (Sigma, St. Louis, MO, USA), CpD α was purchased from Enzo Life Sciences (Farmingdale, NY, USA), and KPT was purchased from Cayman Chemical (Ann Arbor, MI, USA). The aforementioned compounds were dissolved in 100% ethanol (EtOH) and stored at -20°C. BSA-Cort was purchased from MyBioSource (San Diego, CA, USA) and dissolved in sterile water and stored at -20°C. Unconjugated BSA was purchased from Sigma and dissolved in sterile water and stored at

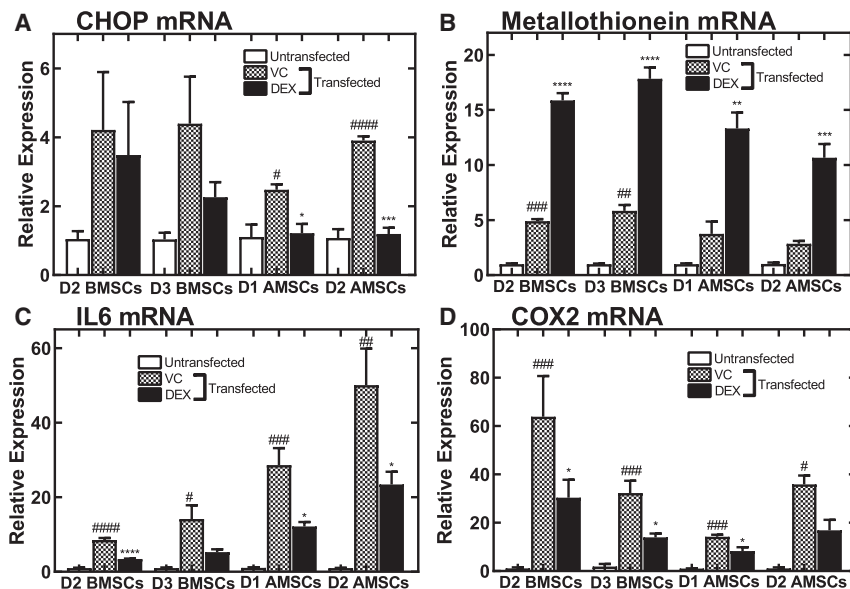


Figure 6. Transfection and DEX Priming Modulates Endogenous hMSC Genes

(A–D) Transfection and DEX priming modulates expression of genes related to endoplasmic reticulum (ER) stress, apoptosis, oxidative stress, and inflammation in hMSCs, as quantified by qRT-PCR 24 h after transfection. In D2 BMSCs, D3 BMSCs, D1 AMSCs, and D2 AMSCs: (A) ER stress-induced and apoptosis mediator CCAAT-enhancer-binding protein homologous protein (CHOP) messenger RNA (mRNA) was upregulated by transfection when treated with only VC and downregulated by DEX treatment when transfected relative to VC; (B) antioxidant protein metallothionein mRNA was upregulated by transfection when treated with VC and further upregulated by transfection with DEX; (C) inflammatory cytokine interleukin-6 (IL-6) mRNA was upregulated by transfection when treated with VC and downregulated by DEX treatment when transfected relative to VC; and (D) inflammatory enzyme cyclooxygenase-2 (COX2) mRNA was upregulated by transfection when treated with VC and downregulated by DEX treatment when transfected relative to VC. Data are plotted as mean \pm SEM ($n = 3$). Pound symbols denote significance to untransfected conditions: # $p \leq 0.05$; ## $p \leq 0.01$; ### $p \leq 0.001$; #### $p \leq 0.0001$. Asterisks denote significance to VC conditions: * $p \leq 0.05$; ** $p \leq 0.01$; *** $p \leq 0.001$; **** $p \leq 0.0001$.

–20°C. For delivery to cells, DEX, Cort, CpdA, and KPT were diluted in EtOH, while BSA-Cort and unconjugated BSA were diluted in sterile water and delivered to cell-culture media, at <1% total media volume, 25 min prior to the addition of DNA lipoplexes. EtOH was delivered as a VC in place of DEX, Cort, CpdA, and KPT. As a control for BSA-Cort, Cort was delivered along with an equal amount of unconjugated BSA in water.

Transfections

pEGFP-Luc plasmid DNA was purchased from Clontech (Mountain View, CA, USA), and the plasmid encodes a fusion protein of EGFP and Luc under the direction of a cytomegalovirus (CMV) promoter and containing simian virus 40 (SV40) enhancer. The plasmid is non-integrating, producing transient transfection. Plasmids were purified from *E. coli* bacteria using QIAGEN reagents (Valencia, CA, USA) and stored in Tris-EDTA (TE) buffer solution (10 mM Tris, 1 mM EDTA [pH 7.4]) at –20°C. pDNA complexed with LF transfection reagents (Invitrogen, Carlsbad, CA, USA) was delivered to the cell media in well plates after the priming of cells, as described earlier. All cells were transfected with LF 3000 except BMSCs that were transfected with LF LTX in BSA-Cort priming experiments (Figures 2A and 2B). Lipoplexes were formed with LF LTX or LF 3000 in serum-free Opti-MEM media (Invitrogen) following the manufacturer's instructions and as noted in the text. Amounts of DNA and DNA:lipid ratios were optimized to allow for high transfection and low toxicity. All transfections were performed with 0.2 μ g pDNA per square centimeter of cell growth area and a DNA:lipid ratio of 1:2, formed in Opti-MEM for 10 min following the manufacturer's instructions. The size and zeta potential of the DNA lipoplexes were determined by dynamic light scattering and laser doppler micro-electrophoresis, respectively, using a Zetasizer Nano ZS90 (Malvern Instruments, Malvern, Worcester-

shire, UK). Size measurements were taken at 25°C at a scattering angle of 90°, and size was reported as the Z-average diameter, in nanometers (d.nm). Zeta potential measurements were also taken at 25°C using folded capillary cells with the measurement mode set to automatic, and the values were reported in millivolts ($n = 3$). Media were changed 3 h after transfection in all experiments except BSA-Cort priming experiments (Figure 2). Experiments with free DNA were not included, as free DNA is generally considered impermeable to cells *in vitro*, requiring cationic polymers or lipids to condense DNA and facilitate cellular uptake and transfection.²⁷

Transfection Assessment

Fluorescence and phase microscopy was conducted 48 h after lipoplex delivery to qualitatively assess cell health and EGFP expression using a Leica DMI 3000B fluorescence microscope (Leica Microsystems, Wetzlar, Germany). For quantification of transfection efficiency, cell nuclei were stained with 1 μ g/mL Hoechst 33342 (Sigma), and cells were then imaged using the Cytation 1 Cell Imaging System (Bio-Tek Instruments, Winooski, VT, USA) configured with a 4 \times objective and light cubes for DAPI (nuclei stain) and GFP (transfected reporter). After image preprocessing and deconvolution to subtract background fluorescence from captured digital images, Gen5 software (BioTek) object analysis was used to determine the number of cells from DAPI images and to determine number and signal intensities of GFP+ cells. Analysis identified objects in both channels by their fluorescence with a minimum and maximum size selection of 10 μ m and 100 μ m, respectively. DAPI and GFP intensity thresholds of 4,000 and 1,500 relative fluorescent units (RFUs) were used, respectively. Transfection efficiency was calculated by dividing the number of GFP objects by number of DAPI objects. After microscopy, cells were washed with PBS and lysed with 1 \times reporter lysis buffer

(Promega, Madison, WI, USA) and stored at -80°C . Transgenic luciferase activity levels were quantified by measuring luciferase luminescence in RLUs with a Luciferase Assay Kit (Promega) and a luminometer (Turner Designs, Sunnyvale, CA, USA). RLUs were normalized to total protein amount determined with a Pierce BCA protein colorimetric assay (Pierce, Rockford, IL, USA) using the DU730 UV-Vis spectrophotometer (Beckman-Coulter, Brea, CA, USA) to measure absorbance at 562 nm. Plotted fold changes for an experimental condition were calculated by dividing each treatment condition replicate value by each control replicate value.

Oxidative Stress Assays

Forty-eight hours after priming and transfection, as described earlier, cell nuclei were stained with $1\ \mu\text{g}/\text{mL}$ Hoechst 33342 (Sigma), and cellular ROSs were stained with CellROX Deep Red Reagent (Invitrogen) following the manufacturer's protocol. Cells were then imaged using the Cytation 1 Cell Imaging System (BioTek) configured with a $4\times$ objective and light cubes for DAPI (nuclei stain) and red fluorescent protein (RFP) (ROS stain). After image preprocessing and deconvolution to subtract background fluorescence from captured digital images, Gen5 software (BioTek) object analysis was used to determine the number of cells from DAPI images and to determine the number and signal intensities of ROS-positive cells. Analysis identified objects in both channels by their fluorescence with a minimum and maximum size selection of $10\ \mu\text{m}$ and $100\ \mu\text{m}$, respectively. DAPI and RFP intensity thresholds of 4,000 and 5,000 RFUs were used, respectively. The proportion of cells experiencing oxidative stress was calculated by dividing number of RFP objects by number of DAPI objects.

mRNA Quantification Studies

To quantify relative mRNA transcript copy numbers of selected genes, 24 h after BMSC and AMSC transfection with the LF 3000 as described earlier, cell lysate was prepared using the SingleShot Cell Lysis Kit (Bio-Rad, Hercules, CA, USA), and RNA was reverse transcribed using the iScript cDNA Kit (Bio-Rad). qRT-PCR was performed on a QuantStudio 6 Flex Real-Time PCR System (Thermo) with Power SYBR Green Master Mix (Thermo Fisher Scientific), and expression was calculated by the $\Delta\Delta\text{Ct}$ method normalizing to endogenous controls RPL13A and HPRT1. See Table S2 for primer sequences (Integrated DNA Technologies).

Statistics

All experiments were performed in triplicate ($n = 3$) on duplicate days in both AMSCs and BMSCs derived from multiple human donors, as noted in the figures. All values are reported as mean \pm standard error of the mean (SEM). Comparative analyses were completed using one-way analysis of variance (ANOVA) with Bonferroni post-test or unpaired t test, where appropriate. Statistical difference was considered at $*p \leq 0.05$, $**p \leq 0.01$, $***p \leq 0.001$, and $****p \leq 0.0001$. Statistics and fold changes highlighted within figures are for treated versus control groups. All statistics were evaluated using Prism GraphPad software (GraphPad Software, La Jolla, CA, USA).

SUPPLEMENTAL INFORMATION

Supplemental Information can be found online at <https://doi.org/10.1016/j.omtm.2020.07.014>.

AUTHOR CONTRIBUTIONS

Conceptualization, A.H. and A.K.P.; Methodology, A.H.; Investigation, A.H., T.K., and K.B.; Writing – Original Draft, A.H.; Writing – Review & Editing, A.H. and A.K.P.; Funding Acquisition, A.K.P.

CONFLICT OF INTERESTS

The authors declare no competing interests.

ACKNOWLEDGMENTS

We would like to thank the National Institutes of Health (1 DP2 EB025760-01), the National Science Foundation (CAREER CBET-1254415), and USDA CSREES-Nebraska (NEB-21-146) for funding. Some of the materials used in this work were provided by the Texas A&M Health Science Center College of Medicine Institute for Regenerative Medicine at Scott & White through a grant from NCRP of the NIH (P40RR017447). Some of this work used services in the Biomedical and Obesity Research Core (BORC) in the Nebraska Center for Prevention of Obesity Diseases (NPOD), which receives partial support from an NIH (NIGMS) COBRE IDeA award (1P20GM104320). The contents of this publication are the sole responsibility of the authors and do not necessarily represent the official views of the NIH or NIGMS.

REFERENCES

- Chamberlain, G., Fox, J., Ashton, B., and Middleton, J. (2007). Concise review: mesenchymal stem cells: their phenotype, differentiation capacity, immunological features, and potential for homing. *Stem Cells* 25, 2739–2749.
- Maxson, S., Lopez, E.A., Yoo, D., Danilkovitch-Miagkova, A., and Leroux, M.A. (2012). Concise review: role of mesenchymal stem cells in wound repair. *Stem Cells Transl. Med.* 1, 142–149.
- Singer, N.G., and Caplan, A.I. (2011). Mesenchymal stem cells: mechanisms of inflammation. *Annu. Rev. Pathol.* 6, 457–478.
- Ren, G., Zhang, L., Zhao, X., Xu, G., Zhang, Y., Roberts, A.I., Zhao, R.C., and Shi, Y. (2008). Mesenchymal stem cell-mediated immunosuppression occurs via concerted action of chemokines and nitric oxide. *Cell Stem Cell* 2, 141–150.
- Baksh, D., Song, L., and Tuan, R.S. (2004). Adult mesenchymal stem cells: characterization, differentiation, and application in cell and gene therapy. *J. Cell. Mol. Med.* 8, 301–316.
- Ryan, J.M., Barry, F.P., Murphy, J.M., and Mahon, B.P. (2005). Mesenchymal stem cells avoid allogeneic rejection. *J. Inflamm. (Lond.)* 2, 8.
- Jacobs, S.A., Roobrouck, V.D., Verfaillie, C.M., and Van Gool, S.W. (2013). Immunological characteristics of human mesenchymal stem cells and multipotent adult progenitor cells. *Immunol. Cell Biol.* 91, 32–39.
- D'souza, N., Rossignoli, F., Golinelli, G., Grisendi, G., Spano, C., Candini, O., Osturu, S., Catani, F., Paolucci, P., Horwitz, E.M., and Dominici, M. (2015). Mesenchymal stem/stromal cells as a delivery platform in cell and gene therapies. *BMC Med.* 13, 186.
- Richardson, S.M., Hoyland, J.A., Mobasheri, R., Csaki, C., Shakibaei, M., and Mobasheri, A. (2010). Mesenchymal stem cells in regenerative medicine: opportunities and challenges for articular cartilage and intervertebral disc tissue engineering. *J. Cell. Physiol.* 222, 23–32.
- Hamann, A., Nguyen, A., and Pannier, A.K. (2019). Nucleic acid delivery to mesenchymal stem cells: a review of nonviral methods and applications. *J. Biol. Eng.* 13, 7.

11. Tang, Y.L., Tang, Y., Zhang, Y.C., Qian, K., Shen, L., and Phillips, M.I. (2005). Improved graft mesenchymal stem cell survival in ischemic heart with a hypoxia-regulated heme oxygenase-1 vector. *J. Am. Coll. Cardiol.* *46*, 1339–1350.
12. Baldari, S., Di Rocco, G., Piccoli, M., Pozzobon, M., Muraca, M., and Toietta, G. (2017). Challenges and Strategies for Improving the Regenerative Effects of Mesenchymal Stromal Cell-Based Therapies. *Int. J. Mol. Sci.* *18*, 2087.
13. Cheng, Z., Ou, L., Zhou, X., Li, F., Jia, X., Zhang, Y., Liu, X., Li, Y., Ward, C.A., Melo, L.G., and Kong, D. (2008). Targeted migration of mesenchymal stem cells modified with CXCR4 gene to infarcted myocardium improves cardiac performance. *Mol. Ther.* *16*, 571–579.
14. Huang, J., Zhang, Z., Guo, J., Ni, A., Deb, A., Zhang, L., Mirosou, M., Pratt, R.E., and Dzau, V.J. (2010). Genetic modification of mesenchymal stem cells overexpressing CCR1 increases cell viability, migration, engraftment, and capillary density in the injured myocardium. *Circ. Res.* *106*, 1753–1762.
15. Kumar, S., and Ponnazhagan, S. (2007). Bone homing of mesenchymal stem cells by ectopic α 4 integrin expression. *FASEB J.* *21*, 3917–3927.
16. Tsuchiya, H., Kitoh, H., Sugiura, F., and Ishiguro, N. (2003). Chondrogenesis enhanced by overexpression of sox9 gene in mouse bone marrow-derived mesenchymal stem cells. *Biochem. Biophys. Res. Commun.* *301*, 338–343.
17. Alberton, P., Popov, C., Prägert, M., Kohler, J., Shukunami, C., Schieker, M., and Docheva, D. (2012). Conversion of human bone marrow-derived mesenchymal stem cells into tendon progenitor cells by ectopic expression of scleraxis. *Stem Cells Dev.* *21*, 846–858.
18. Beegle, J.R., Magner, N.L., Kalomoiris, S., Harding, A., Zhou, P., Nacey, C., White, J.L., Pepper, K., Gruenloh, W., Annett, G., et al. (2016). Preclinical evaluation of mesenchymal stem cells overexpressing VEGF to treat critical limb ischemia. *Mol. Ther. Methods Clin. Dev.* *3*, 16053.
19. Pollock, K., Dahlenburg, H., Nelson, H., Fink, K.D., Cary, W., Hendrix, K., Annett, G., Torrest, A., Deng, P., Gutierrez, J., et al. (2016). Human mesenchymal stem cells genetically engineered to overexpress brain-derived neurotrophic factor improve outcomes in Huntington's disease mouse models. *Mol. Ther.* *24*, 965–977.
20. Choi, J.J., Yoo, S.A., Park, S.J., Kang, Y.J., Kim, W.U., Oh, I.H., and Cho, C.S. (2008). Mesenchymal stem cells overexpressing interleukin-10 attenuate collagen-induced arthritis in mice. *Clin. Exp. Immunol.* *153*, 269–276.
21. Nakajima, M., Nito, C., Sowa, K., Suda, S., Nishiyama, Y., Nakamura-Takahashi, A., Nitahara-Kasahara, Y., Imagawa, K., Hirato, T., Ueda, M., et al. (2017). Mesenchymal stem cells overexpressing interleukin-10 promote neuroprotection in experimental acute ischemic stroke. *Mol. Ther. Methods Clin. Dev.* *6*, 102–111.
22. Yu, B., Kim, H.W., Gong, M., Wang, J., Millard, R.W., Wang, Y., Ashraf, M., and Xu, M. (2015). Exosomes secreted from GATA-4 overexpressing mesenchymal stem cells serve as a reservoir of anti-apoptotic microRNAs for cardioprotection. *Int. J. Cardiol.* *182*, 349–360.
23. Baglio, S.R., Rooijers, K., Koppers-Lalic, D., Verweij, F.J., Pérez Lanzón, M., Zini, N., Naaijkens, B., Perut, F., Niessen, H.W., Baldini, N., and Pegtel, D.M. (2015). Human bone marrow- and adipose-mesenchymal stem cells secrete exosomes enriched in distinctive miRNA and tRNA species. *Stem Cell Res. Ther.* *6*, 127.
24. Oggu, G.S., Sasikumar, S., Reddy, N., Ella, K.K.R., Rao, C.M., and Bokara, K.K. (2017). Gene delivery approaches for mesenchymal stem cell therapy: strategies to increase efficiency and specificity. *Stem Cell Rev. Rep.* *13*, 725–740.
25. Nayerossadat, N., Maedeh, T., and Ali, P.A. (2012). Viral and nonviral delivery systems for gene delivery. *Adv. Biomed. Res.* *1*, 27.
26. Yin, H., Kanasty, R.L., Eltoukhy, A.A., Vegas, A.J., Dorkin, J.R., and Anderson, D.G. (2014). Non-viral vectors for gene-based therapy. *Nat. Rev. Genet.* *15*, 541–555.
27. Jin, L., Zeng, X., Liu, M., Deng, Y., and He, N. (2014). Current progress in gene delivery technology based on chemical methods and nano-carriers. *Theranostics* *4*, 240–255.
28. Hoare, M., Greiser, U., Schu, S., Mashayekhi, K., Aydogan, E., Murphy, M., Barry, F., Ritter, T., and O'Brien, T. (2010). Enhanced lipoplex-mediated gene expression in mesenchymal stem cells using reiterated nuclear localization sequence peptides. *J. Gene Med.* *12*, 207–218.
29. Madeira, C., Mendes, R.D., Ribeiro, S.C., Boura, J.S., Aires-Barros, M.R., da Silva, C.L., and Cabral, J.M. (2010). Nonviral gene delivery to mesenchymal stem cells using cationic liposomes for gene and cell therapy. *J. Biomed. Biotechnol.* *2010*, 735349.
30. Ribeiro, S.C., Mendes, R., Madeira, C., Monteiro, G.A., da Silva, C.L., and Cabral, J.M. (2010). A quantitative method to evaluate mesenchymal stem cell lipofection using real-time PCR. *Biotechnol. Prog.* *26*, 1501–1504.
31. Peng, L., Gao, Y., Xue, Y.-N., Huang, S.-W., and Zhuo, R.-X. (2013). The effectiveness, cytotoxicity, and intracellular trafficking of nonviral vectors for gene delivery to bone mesenchymal stem cells. *J. Bioact. Compat. Polym.* *28*, 204–217.
32. Ahn, H.H., Lee, J.H., Kim, K.S., Lee, J.Y., Kim, M.S., Khang, G., Lee, I.W., and Lee, H.B. (2008). Polyethyleneimine-mediated gene delivery into human adipose derived stem cells. *Biomaterials* *29*, 2415–2422.
33. Wang, W., Li, W., Ou, L., Flick, E., Mark, P., Nesselmann, C., Lux, C.A., Katzen, H.H., Kaminski, A., Liebold, A., et al. (2011). Polyethylenimine-mediated gene delivery into human bone marrow mesenchymal stem cells from patients. *J. Cell. Mol. Med.* *15*, 1989–1998.
34. Corsi, K., Chellat, F., Yahia, L., and Fernandes, J.C. (2003). Mesenchymal stem cells, MG63 and HEK293 transfection using chitosan-DNA nanoparticles. *Biomaterials* *24*, 1255–1264.
35. King, W.J., Kouris, N.A., Choi, S., Ogle, B.M., and Murphy, W.L. (2012). Environmental parameters influence non-viral transfection of human mesenchymal stem cells for tissue engineering applications. *Cell Tissue Res.* *347*, 689–699.
36. Nguyen, A., Beyersdorf, J., Riethoven, J.J., and Pannier, A.K. (2016). High-throughput screening of clinically approved drugs that prime polyethylenimine transfection reveals modulation of mitochondria dysfunction response improves gene transfer efficiencies. *Bioeng. Transl. Med.* *1*, 123–135.
37. Martin, T.M., Plautz, S.A., and Pannier, A.K. (2015). Temporal endogenous gene expression profiles in response to lipid-mediated transfection. *J. Gene Med.* *17*, 14–32.
38. Martin, T.M., Plautz, S.A., and Pannier, A.K. (2015). Temporal endogenous gene expression profiles in response to polymer-mediated transfection and profile comparison to lipid-mediated transfection. *J. Gene Med.* *17*, 33–53.
39. Kelly, A.M., Plautz, S.A., Zempleni, J., and Pannier, A.K. (2016). Glucocorticoid Cell Priming Enhances Transfection Outcomes in Adult Human Mesenchymal Stem Cells. *Mol. Ther.* *24*, 331–341.
40. Hamann, A., Broad, K., Nguyen, A., and Pannier, A.K. (2019). Mechanisms of unprimed and dexamethasone-primed nonviral gene delivery to human mesenchymal stem cells. *Biotechnol. Bioeng.* *116*, 427–443.
41. Strehl, C., Gaber, T., Löwenberg, M., Hommes, D.W., Verhaar, A.P., Schellmann, S., Hahne, M., Fangradt, M., Wagegg, M., Hoff, P., et al. (2011). Origin and functional activity of the membrane-bound glucocorticoid receptor. *Arthritis Rheum.* *63*, 3779–3788.
42. Roberson, S., Allie-Reid, F., Vanden Berghe, W., Visser, K., Binder, A., Africander, D., Vismser, M., De Bosscher, K., Hapgood, J., Haegeman, G., and Louw, A. (2010). Abrogation of glucocorticoid receptor dimerization correlates with dissociated glucocorticoid behavior of compound a. *J. Biol. Chem.* *285*, 8061–8075.
43. Kashyap, T., Klebanov, B., Lee, M.S., and Landesman, Y. (2015). Selinexor, a selective inhibitor of nuclear export (SINE) compound, shows synergistic anti-tumor activity in combination with dexamethasone characterized by specific pattern of gene expression in multiple myeloma (MM). *Blood* *126*, 3683.
44. Vernocchi, S., Battello, N., Schmitz, S., Revets, D., Billing, A.M., Turner, J.D., and Muller, C.P. (2013). Membrane glucocorticoid receptor activation induces proteomic changes aligning with classical glucocorticoid effects. *Mol. Cell. Proteomics* *12*, 1764–1779.
45. Ayrout, M., Simon, V., Bernard, V., Binart, N., Cohen-Tannoudji, J., Lombès, M., and Chauvin, S. (2017). A novel non genomic glucocorticoid signaling mediated by a membrane palmitoylated glucocorticoid receptor cross talks with GnRH in gonadotrope cells. *Sci. Rep.* *7*, 1537.
46. Strehl, C., and Buttgerit, F. (2014). Unraveling the functions of the membrane-bound glucocorticoid receptors: first clues on origin and functional activity. *Ann. N Y Acad. Sci.* *1318*, 1–6.

47. Choi, J.-S., and Lee, M.-H. (2005). Effect of dexamethasone preincubation on polymer-mediated gene delivery. *Bull. Korean Chem. Soc.* *26*, 1209–1213.
48. Dewint, P., Gossye, V., De Bosscher, K., Vanden Berghe, W., Van Beneden, K., Deforce, D., Van Calenbergh, S., Müller-Ladner, U., Vander Cruyssen, B., Verbruggen, G., et al. (2008). A plant-derived ligand favoring monomeric glucocorticoid receptor conformation with impaired transactivation potential attenuates collagen-induced arthritis. *J. Immunol.* *180*, 2608–2615.
49. Lesovaya, E., Yemelyanov, A., Swart, A.C., Swart, P., Haegeman, G., and Budunova, I. (2015). Discovery of Compound A—a selective activator of the glucocorticoid receptor with anti-inflammatory and anti-cancer activity. *Oncotarget* *6*, 30730–30744.
50. Martin, T.M., Plautz, S.A., and Pannier, A.K. (2013). Network analysis of endogenous gene expression profiles after polyethyleneimine-mediated DNA delivery. *J. Gene Med.* *15*, 142–154.
51. Lonez, C., Vandenbranden, M., and Ruyschaert, J.-M. (2012). Cationic lipids activate intracellular signaling pathways. *Adv. Drug Deliv. Rev.* *64*, 1749–1758.
52. Kongkanermit, L., Sarisuta, N., Azad, N., Lu, Y., Iyer, A.K.V., Wang, L., and Rojanasakul, Y. (2008). Dependence of reactive oxygen species and FLICE inhibitory protein on lipofectamine-induced apoptosis in human lung epithelial cells. *J. Pharmacol. Exp. Ther.* *325*, 969–977.
53. Lee, M.S., Kim, N.W., Lee, K., Kim, H., and Jeong, J.H. (2013). Enhanced transfection by antioxidative polymeric gene carrier that reduces polyplex-mediated cellular oxidative stress. *Pharm. Res.* *30*, 1642–1651.
54. Cao, S.S., and Kaufman, R.J. (2014). Endoplasmic reticulum stress and oxidative stress in cell fate decision and human disease. *Antioxid. Redox Signal.* *21*, 396–413.
55. Zhang, K., and Kaufman, R.J. (2008). From endoplasmic-reticulum stress to the inflammatory response. *Nature* *454*, 455–462.
56. Tabas, I., and Ron, D. (2011). Integrating the mechanisms of apoptosis induced by endoplasmic reticulum stress. *Nat. Cell Biol.* *13*, 184–190.
57. Nishitoh, H. (2012). CHOP is a multifunctional transcription factor in the ER stress response. *J. Biochem.* *151*, 217–219.
58. Yoon, Y.M., Lee, J.H., Yun, S.P., Han, Y.-S., Yun, C.W., Lee, H.J., Noh, H., Lee, S.J., Han, H.J., and Lee, S.H. (2016). Tauroursodeoxycholic acid reduces ER stress by regulating of Akt-dependent cellular prion protein. *Sci. Rep.* *6*, 39838.
59. Wei, H., Li, Z., Hu, S., Chen, X., and Cong, X. (2010). Apoptosis of mesenchymal stem cells induced by hydrogen peroxide concerns both endoplasmic reticulum stress and mitochondrial death pathway through regulation of caspases, p38 and JNK. *J. Cell. Biochem.* *111*, 967–978.
60. Das, I., Png, C.W., Oancea, I., Hasnain, S.Z., Lourie, R., Proctor, M., Eri, R.D., Sheng, Y., Crane, D.I., Florin, T.H., and McGuckin, M.A. (2013). Glucocorticoids alleviate intestinal ER stress by enhancing protein folding and degradation of misfolded proteins. *J. Exp. Med.* *210*, 1201–1216.
61. Fujii, Y., Khoshnoodi, J., Takenaka, H., Hosoyamada, M., Nakajo, A., Bessho, F., Kudo, A., Takahashi, S., Arimura, Y., Yamada, A., et al. (2006). The effect of dexamethasone on defective nephrin transport caused by ER stress: a potential mechanism for the therapeutic action of glucocorticoids in the acquired glomerular diseases. *Kidney Int.* *69*, 1350–1359.
62. Mihailidou, C., Panagiotou, C., Kiaris, H., Kassi, E., and Moutsatsou, P. (2016). Crosstalk between C/EBP homologous protein (CHOP) and glucocorticoid receptor in lung cancer. *Mol. Cell. Endocrinol.* *436*, 211–223.
63. Qian, Y., Jing, Y., and Li, Z.J. (2010). Glucocorticoid receptor-mediated reduction of IgG-fusion protein aggregation in Chinese hamster ovary cells. *Biotechnol. Prog.* *26*, 1417–1423.
64. Ruttkey-Nedecky, B., Nejdil, L., Gumulec, J., Zitka, O., Masarik, M., Eckschlager, T., Stiborova, M., Adam, V., and Kizek, R. (2013). The role of metallothionein in oxidative stress. *Int. J. Mol. Sci.* *14*, 6044–6066.
65. Hasnain, S.Z., Lourie, R., Das, I., Chen, A.C.H., and McGuckin, M.A. (2012). The interplay between endoplasmic reticulum stress and inflammation. *Immunol. Cell Biol.* *90*, 260–270.
66. Gargalovic, P.S., Gharavi, N.M., Clark, M.J., Pagnon, J., Yang, W.-P., He, A., Truong, A., Baruch-Oren, T., Berliner, J.A., Kirchgessner, T.G., and Lusis, A.J. (2006). The unfolded protein response is an important regulator of inflammatory genes in endothelial cells. *Arterioscler. Thromb. Vasc. Biol.* *26*, 2490–2496.
67. Cao, S.S., Luo, K.L., and Shi, L. (2016). Endoplasmic reticulum stress interacts with inflammation in human diseases. *J. Cell. Physiol.* *231*, 288–294.
68. Chaudhari, N., Talwar, P., Parimisetty, A., Lefebvre d'Helencourt, C., and Ravanan, P. (2014). A molecular web: endoplasmic reticulum stress, inflammation, and oxidative stress. *Front. Cell. Neurosci.* *8*, 213.